Structural, bacteriostatic and antioxidant profiling of zinc oxide nanoparticles

H. Azeem[a], S. U. Rehman[a], S. Haq[a,*], S. U. Din[a], Kh. Elmnasri[b], M. Ben Ali[c], Kh. Elhadef[d], A. Hedfi[c], J. Razzokov [e,g], E. Mahmoudi[h]
[a]*Department of Chemistry, University of Azad Jammu and Kashmir, Muzaffarabad 13100, Pakistan*
[b]*Laboratory of bacteriological research, Institute of veterinary research of Tunisia, University of Tunis El Manar, Tunis 1006, Tunisia*
[c]*Department of Biology, College of Sciences, Taif University, PO Box 11099, Taif 21944, Saudi Arabia*
[d]*Laboratory of Microbial Biotechnology and Engineering Enzymes (LMBEE), Center of Biotechnology of Sfax 7 (CBS), University of Sfax, Sfax, Tunisia*
[e]*Institute of Fundamental and Applied Research, National Research University TIIAME, Kori Niyoziy 39, 100000 Tashkent, Uzbekistan*
[f]*Laboratory of Experimental Biophysics, Centre for Advanced Technologies, Universitet 7, Tashkent 100174, Uzbekistan*
[g]*Department of Biomedical Engineering, Tashkent State Technical University, Tashkent 100095, Uzbekistan*
[h]*Coastal Ecology and Ecotoxicology Unit, LR01ES14 Laboratory of Environment Biomonitoring, Faculty of Sciences of Bizerte, University of Carthage, 7021 Zarzouna, Tunisia*

The bacterial infection and generation of free radicals inside the body are serious threats to human health globally and researchers show their serious concern for these issues. Thus, in this study, an attempt has been made to control bacterial growth and scavenge the ABTs free radicals. ZnO-NPs were synthesized by an economical method, and the characteristics were investigated using a range of analytical techniques. These methods included FTIR, SEM, EDX, XRD, and TEM. The agar-well diffusion process has been followed to control the growth of selected bacteria and the ABTs free radicals have been scavenged using a standard protocol. The effect of the dose on both activities has been studied where the results has explore that the effectiveness of the ZnO-NPs gradually increases with increasing concentration.

(Received January 17, 2024; Accepted April 22, 2024)

Keywords: Zinc oxide, Characterization, Antioxidant, Antibacterial agent

1. Introduction

Multi-drug resistant bacteria (MDR) are strains of bacteria that have developed resistance to multiple antibiotics. This poses a significant public health concern as it makes treatment of infections, caused by these bacteria, much more difficult [1]. Metal oxide nanoparticles (MO-NPs) have been studied as potential tools for combating MDR bacteria due to their unique physicochemical properties [2]. Investigation has indicated that MONPs exhibit significant inhibition against multidrug-resistant (MDR) bacteria. The mechanism underlying this phenomenon is believed to involve the interaction among the nanoparticles and the bacterial membrane [3]. The enhanced surface area as compared to volume of MO-NPs enables them to interact more efficiently with the bacterial cell membrane, disrupting its integrity and ultimately causing the destruction of the organism [4].

The ZnO is a semiconductor known for its affordable cost and possesses a band gap energy of 3.37 eV. It has garnered significant attention due to its distinctive characteristics and

* Corresponding authors: cii_raj@yahoo.com
https://doi.org/10.15251/DJNB.2024.192.661

promising applications across multiple domains [5]. ZnO typically exists in two forms: hexagonal wurtzite and cubic zinc blend [6]. The ZnO-NPs are less than 100 nanometers in size and exhibit enhanced properties such as increased surface area, higher reactivity, and unique optical as well as electronic properties compared to their bulk counterparts [7,8]. These properties make ZnO-NPs attractive for usage in electronics, medicine, cosmetics, and textiles [9,10]. Besides this, ZnO-NPs had gained attention because of their biological efficacy and showing promising activities in fields such as medicine, biotechnology, and agriculture [11,12].

This research study was conducted to apply a user friendly and economical process for the preparation of ZnO-NPs. Various techniques, including XRD, SEM, TEM, EDX, and FTIR, were employed to examine the ZnO NPs shape, content, and functional groups. Furthermore, tests for antioxidant and antibacterial properties were performed to evaluate the possible uses of ZnO-NPs. The individual techniques used in our study may have been previously explored; however, this manuscript has presented a comprehensive investigation that combines structural, bacteriostatic, and antioxidant profiling of Zinc Oxide nanoparticles in a single study. This holistic approach provides a deeper understanding of the nanoparticles' multifaceted potentials, their interplay, and how they collectively contribute to their overall efficacy.

2. Research procedure

2.1. Reagents used

The regents used are $ZnCl_2.2H_2O$, KOH, agar nutrients, ABTs, ethanol and distilled water.

2.2. Formation of ZnO-NPs

In a titration flask, a solution containing 80 mL of $ZnCl_2.2H_2O$ (40 mM) was made and mixed with 15 mL of ethanol. Stirring constantly, the mixture was heated for 20 minutes at 60°C on a hot plate. After that, the reaction mixture was gradually mixed with 5 mL of 1 M KOH solution dropwise until a pH of 10 was reached. For half an hour more, the reaction was agitated under heating condition. After the synthesized ZnO-NPs were finished, the supernatant was decanted and allowed to settle. The final product washed three times in a row in warm distilled water. At the end, the product was dried at 100 °C in an oven and storing it properly for the next round of experiments.

2.3. Instrumentation

The crystal structure, surface morphology as well as elemental and chemical compositions of ZnO-NPs, were studied by XRD (Panalytical X'pert pro), TEM model JSM-1200, EDX (INCA 200) coupled with SEM, SEM model JSM 5910, and the FTIR (model: Nicolet 6700), respectively [13–15].

2.4. Bactericidal assay

In order to investigate the activity of ZnO-NPs against bacteria using a standard procedure [13]. The bacteria were uniformly spread onto agar plates using sterile swabs, and bore-holes were made, which were equipped with different volumes (ranging from 20 to 100 µL) of NPs dispersion. The NPs dispersion was prepared by sonicating 0.001 g in 0.001 L of DMSO. The plates were incubated at 37°C and after 24 h the clear zone was measure as the activity of NPs.

2.5. ABTs inhibition assay

The antioxidant capability of ZnO-NPs was assessed through the ABTS assay. Initially, 7 mM ABTS with 2.5 mM $K_2S_2O_8$ was combined to prepared a stock solution. Subsequently, the working solution for the nanoparticles was generated by combining equal portions of the two stock solutions, followed by an overnight incubation in dark. The distilled water was added to this solution for dilution to achieve an absorbance reading of 0.45 at 405 nm using a spectrophotometer. Typically, 0.0001 L of ABTS solution was combine with 50-300 µL of nanoparticle solutions, and DMSO was added to attain a total reaction volume of approximately 3 NPs dispersion. The absorbance (Ai) of the reaction mixture was recorded, and the percentage scavenging potential was computed using the provided formula (eq.1):

$$\%\ Scavening\ potential = \frac{(A_o - A_i)}{A_o} \times 100 \quad \text{(eq. 1)}$$

3. Results and Discussion

3.1. XRD analysis

ZnO-NPs X-ray diffractogram (Fig. 1) showed distinct and strong diffraction peaks at different 2θ positions: 31.90°, 34.45°, 36.27°, 47.59°, 56.63°, 62.97°, and 68.11°. The diffraction patterns produced by the corresponding miller planes, especially (100), (002), (101), (102), (110), (103), and (112), were matched by these peaks [16]. These distinctive peaks demonstrated the hexagonal crystal structure of the ZnO NPs and were consistent with reference card 01-079-0205. The crystallite size and lattice strain was found to be 25.84 nm and 0.323%, respectively.

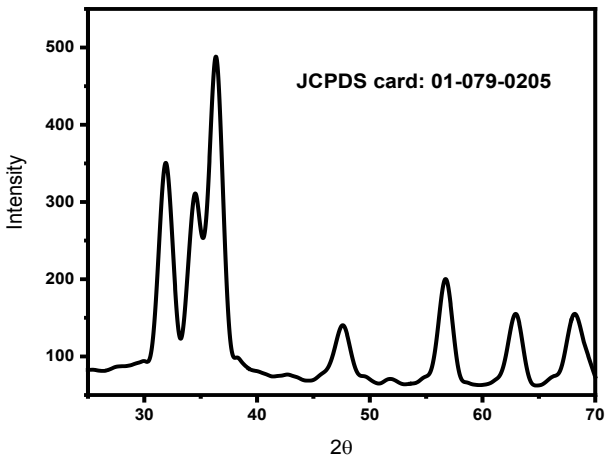

Fig. 1. XRD pattern of ZnO Nanoparticles.

3.2. SEM analysis

As shown in Fig. 2, SEM analysis of the ZnO-NPs was carried out at low and high magnifications. A notable degree of agglomeration was seen in the low magnification SEM image, suggesting the production of big particles on the flat surface. These particles formed an irregular network due to their intimate interconnections. In addition, the particles varied in size and shape, with most of them seeming almost spherical. The average size of the estimated particles was 99.62 nm, and they ranged in size from 88 to 121 nm.

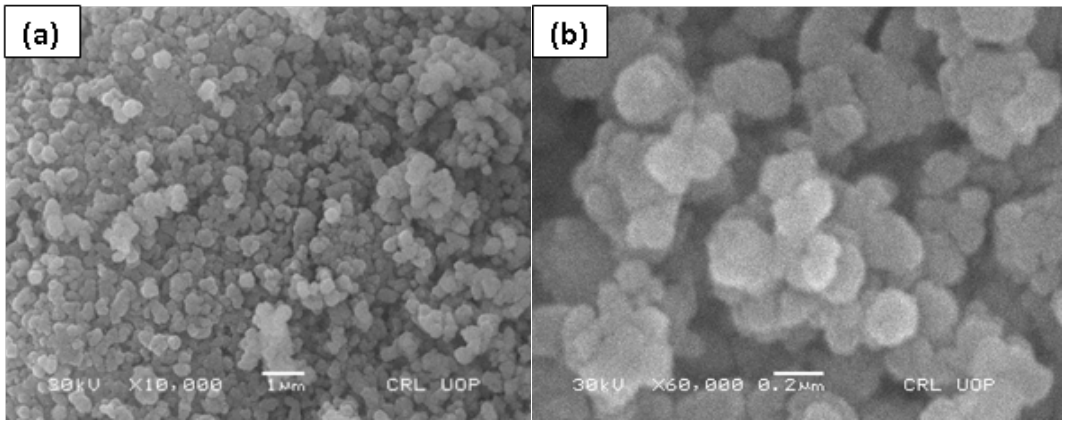

Fig. 2. SEM Images of ZnO Nanoparticles at Low (a) and High (b) Magnifications.

3.3. TEM analysis

The TEM pictures shown in Figure 3, both at low (a) and high (b) magnifications, provide a thorough understanding of the morphology of the prepared NPs. They show a wide variety of particle forms and architectures. The TEM image at low magnification revealed two unique regions: one was where increasing surface energy caused particle fusion, which resulted in the merging of particles and the development of a sheet-like structure. This fusion process was also seen in the TEM image (b) at extreme magnification. In another area, upon closer examination, it was possible to see boundaries between the tightly spaced particles. The particles maintained their unique morphological features in spite of this relationship, even if they lacked distinct forms. Most of the particles in the sample had a roughly spherical appearance, although some had a randomly distributed polyhedral morphology. The particle sizes are ranging from 25 to 60 nm, were also shown by the TEM examination, with the smaller particles getting closer to the ZnO-NPs' crystallite size. Furthermore, compared to the particles seen in the TEM image, the grains seen in the SEM photos looked to be two to three times larger.

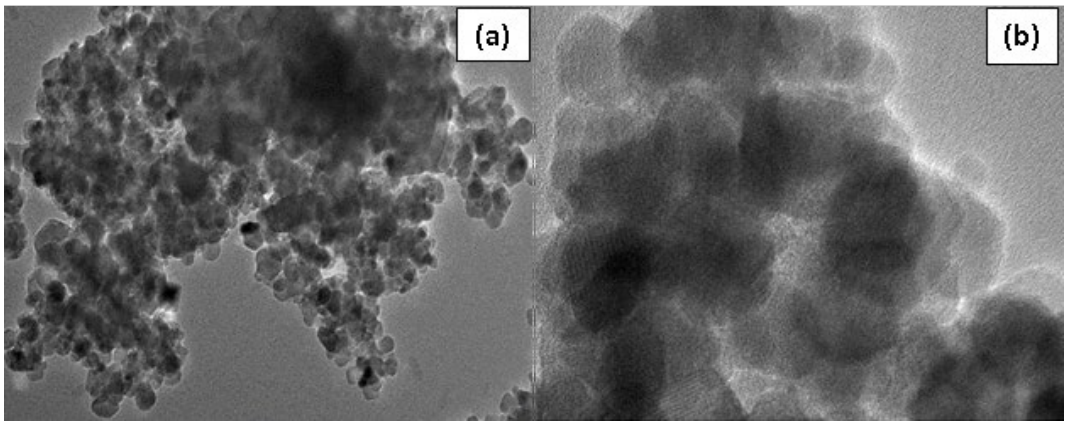

Fig. 3. TEM micrographs (a and b) of ZnO Nanoparticles.

3.4. EDX analysis

The existence of Zn in the sample was evident from the sharp signals at 0.9, 08.70, and 09.60 keV in the Fig. 4. In addition to this, another single at 0.24 keV was attributed to the O in the samples, which revealed the formation of ZnO. Based on the EDX analysis, Zn and O had percent weights of 80.3 and 19.7, respectively. This implied that the sample was predominantly made up of Zn, which was consistent with the preparation of the sample. The investigations further confirmed purity of the sample without any impurities.

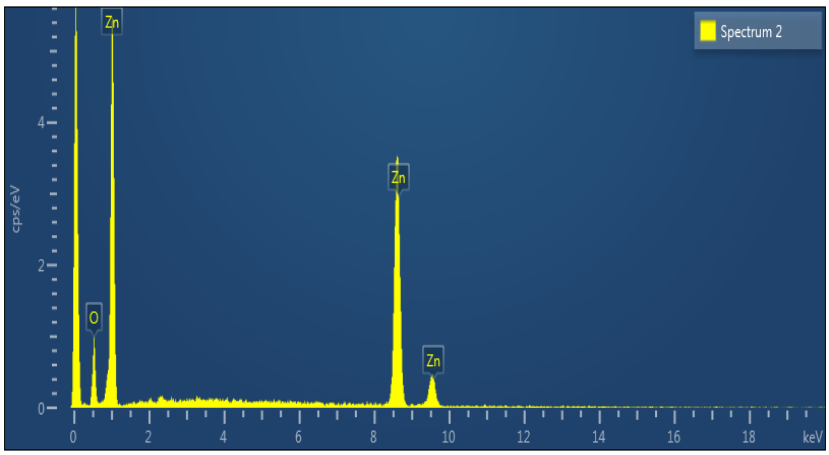

Fig. 4. EDX Analysis of ZnO Nanoparticles.

3.4. FTIR analysis

The extending band of the O-H functional group was visible in the Fig. 5 in the ranges of 3539-3376 cm^{-1} [17]. The O-H functional group bending vibration was visible at 1626.92 cm^{-1}. A sharp peak at 1379.56 cm^{-1} is due to the vibration of M-OH. The peak at 1027.44 cm^{-1} was caused by O-Zn-O extending pulsation within the crystal structure but the bands at 673.71 and 478.33 cm^{-1} were because of Zn-O stretching and bending vibrations [18].

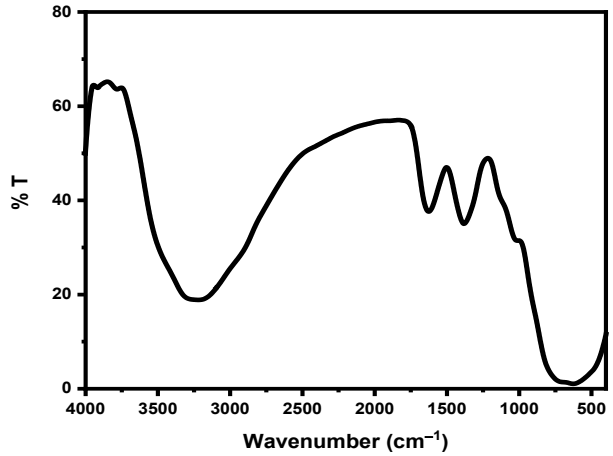

Fig. 5. FTIR Analysis of ZnO Nanoparticles

3.5. Antibacterial analysis

To determine if ZnO-NPs could limit the growth of dangerous strains including *S. aureus* and *E. coli*, which are known to cause serious illnesses, an antibacterial experiment was conducted. Table 1 presents a tabulation of the associated data, whereas Fig. 6 presents the experimental photos. The findings show that as the ZnO suspension concentration in the wells grew, so did the growth inhibitory activity. This implies that ZnO-NPs may be more effective against the tested bacterial strains at higher concentration [19]. ZnO-NPs also showed a stronger growth inhibitory impact against *E. coli* than *S. aureus*. This variance may be explained by the different ways that ZnO-NPs react chemically in aqueous settings as well as the ways that the bacterial strains' outer membranes differ chemically [20,21]. The strong linkage among the Zn^{2+} and *E. coli* surfaces were due to phospholipid and lipopolysaccharide, whereas the week interaction with *S. aureus* was due to the partial negative charge imparted by teichoic acid [20,22].

Table 1. The bactericidal results of ZnO-NPs extracted from the agar well diffusion experiment.

Species		**Volume of ZnO-NPs in µL**				**-ve control**
	20	**40**	**60**	**80**	**100**	
S. aureus	0.5	01	04	07	10	00
E. coli	1	02	07	10	14	00

3.6. Antioxidant analysis

The ABTs radical inhibiting potential of ZnO NPs was evaluated. The percentage RSA of the samples was determined and listed in Table 2. The obtained results were compared with the antioxidant potential of ascorbic acid which had been used as a standard. The study showed a gradual increase with elevating concentrations of both samples in the current experimental procedure. The increase in antioxidant activity at higher concentrations might have been contributed by the larger number of ZnO-NPs that generated more ABTs radicals. At elevated concentrations, more ZnO NPs were available to come into contact with free radicals, which could enhance the scavenging and trapping of free radicals, effectively reducing their levels and preventing further damage to cells and tissues [23].

The maximum activity percentage was reported at 300 µg for ascorbic acid (99.56%) and ZnO-NPs (98.01%). The sample concentration that inhibit 50 percent of the free radicals is terms as IC_{50} and greater effectiveness in scavenging free radicals is indicated by a lower IC_{50} value. The synthesized ZnO-NPs showed considerable antioxidant activity, as indicated by their IC_{50} value of 83.89 µg/µL, which was marginally greater than that of ascorbic acid (77.35 µg/µL)[24].

Table 2. Antioxidant activity of ZnO-NPs against ABTS free radicals.

Sample	Concentration (µg/µL)	Activity (%)	IC_{50} (µg/µL)	Variance (S^2)	STD Dev.
ZnO-NPs	50 100 200 300	40.23 54.02 81.34 98.01	83.89	2.26	1.51
Ascorbic acid	50 100 200 300	41.34 55.78 83.55 99.56	77.35	2.25	1.51

4. Conclusion

This study aimed to synthesize biologically potent ZnO-NPs to address challenges associated with drug-resistant strains and free radical generation. The synthesis process employed a straightforward and cost-effective method applicable to various nanoparticles. The ZnO NPs' strong crystalline structure was confirmed by XRD analysis, and the particle morphology's uneven distribution was shown by SEM observation. The ZnO-NPs were found to have a high degree of purity and elemental composition, with no obvious contaminants. The results showed that the antibacterial activity was more against *E. coli* at higher volumes, perhaps because of differences in cell wall composition. Furthermore, the nanoparticles demonstrated antioxidant efficacy against ABTs free radicals that was dose-dependent.

Acknowledgments

The authors extend their appreciation to Taif University, Saudi Arabia, for supporting this work through project number (TU-DSPP-2024-176).

References

[1] Chen, H.; Zhang, M.; Li, B.; Chen, D.; Dong, X.; Wang, Y.; Gu, Y., Biomaterials 2015, 53, 532-544; https://doi.org/10.1016/j.biomaterials.2015.02.105

[2] Happy Agarwal; Menon, S.; Venkat Kumar, S.; Rajeshkumar, S., Chemico-Biological Interactions 2018, 286, 60-70; https://doi.org/10.1016/j.cbi.2018.03.008

[3] Veerapandian, M.; Yun, K., Applied Microbiology and Biotechnology 2011, 90, 1655-1667; https://doi.org/10.1007/s00253-011-3291-6

[4] Ahamed, M.; Alhadlaq, H. A.; Khan, M. A. M.; Karuppiah, P.; Al-dhabi, N. A. Synthesis, Characterization, and Antimicrobial Activity of Copper Oxide Nanoparticles. 2014, 2014; https://doi.org/10.1155/2014/637858

[5] Jiang, J.; Pi, J.; Cai, J., Bioinorganic Chemistry and Applications 2018, 2018; https://doi.org/10.1155/2018/1062562

[6] Cheng, J.; Wang, P.; Hua, C.; Yang, Y.; Zhang, Z., Materials 2018, 11; https://doi.org/10.3390/ma11030417

[7] Fahimmunisha, B. A.; Ishwarya, R.; AlSalhi, M. S.; Devanesan, S.; Govindarajan, M.; Vaseeharan, B., Journal of Drug Delivery Science and Technology 2020, 55, 101465; https://doi.org/10.1016/j.jddst.2019.101465

[8] Singh, V.; Vishal, M., Journal of Environmental Chemical Engineering 2021, 9, 106279; https://doi.org/10.1016/j.jece.2021.106279

[9] Siddiqi, K. S.; ur Rahman, A.; Tajuddin; Husen, A., Nanoscale Research Letters 2018 13:1 2018, 13, 1-13; https://doi.org/10.1186/s11671-018-2532-3

[10] Wan, Q.; Zhang, Z.; Hou, Z.-W.; Lei, W., Organic Chemistry Frontiers 2023; https://doi.org/10.1039/D3QO00408B

[11] Kumar, V.; Yadav, S. K., Plant-mediated synthesis of silver and gold nanoparticles and their applications. 2009, 176061, 151-157; https://doi.org/10.1002/jctb.2023

[12] Lu, J.; Yi, C.; Ding, M.; Fan, X.; Hu, J.; Chen, Y.; Li, J.; Li, Z.; Liu, W. A., Carbohydrate Polymers 2022, 227, 118871; https://doi.org/10.1016/j.carbpol.2021.118871

[13] Haq, S.; Rehman, W.; Rehman, M., Journal of Inorganic and Organometallic Polymers and Materials 2020, 30, 1197-1205; https://doi.org/10.1007/s10904-019-01256-3

[14] Khan, B.; Nawaz, M.; Waseem, M.; Hussain, R.; Arif, S.; Price, G. J.; Haq, S.; Rehman, W., Materials Research Express 2019, 6; https://doi.org/10.1088/2053-1591/ab2ef9

[15] Luo, H.; Lou, Y.; He, K.; Jiang, Z., Combustion and Flame 2023, 249, 112609; https://doi.org/10.1016/j.combustflame.2022.112609

[16] Bibi, N.; Haq, S.; Rehman, W.; Waseem, M.; Rehman, M. U.; Shah, A.; Khan, B.; Rasheed, P., Biointerface research in applied chemistry 2020, 10, 5895-5900; https://doi.org/10.33263/BRIAC104.895900

[17] Kumar, H.; Rani, R., International Letters of Chemistry, Physics and Astronomy 2013, 19, 26-36; https://doi.org/10.18052/www.scipress.com/ILCPA.19.26

[18] Shoukat, S.; Rehman, W.; Haq, S.; Waseem, M.; Shah, A., Materials Research Express 2019, 6, 115052; https://doi.org/10.1088/2053-1591/ab473c

[19] Haq, S.; Yasin, K. A.; Rehman, W.; Waseem, M.; Ahmed, M. N.; Shahzad, M. I.; Shahzad, N.; Shah, A.; Rehman, M. U.; Khan, B., Journal of Inorganic and Organometallic Polymers and Materials 2020, 31, 1134-1142; https://doi.org/10.1007/s10904-020-01763-8

[20] Shah, A.; Tauseef, I.; Ali, M. Bin; Yameen, M. A.; Mezni, A.; Hedfi, A.; Haleem, S. K.; Haq, S., Toxics 2021, 9, 105-120; https://doi.org/10.3390/toxics9050105

[21] Wang, Y.; Zhai, W.; Cheng, S.; Li, J.; Zhang, H. Friction 2023, 11, 1371-1394; https://doi.org/10.1007/s40544-022-0710-x

[22] Mahfooz-Ur-Rehman, M.; Rehman, W.; Waseem, M.; Shah, B. A.; Shakeel, M.; Haq, S.; Zaman, U.; Bibi, I.; Khan, H. D., Journal of Chemical and Engineering Data 2019, 64, 2436-2444; https://doi.org/10.1021/acs.jced.8b01243

[23] Singh, V.; Singh, N.; Verma, M.; Kamal, R.; Tiwari, R.; Sanjay Chivate, M.; Rai, S. N.;

Kumar, A.; Singh, A.; Singh, M. P.; Vamanu, E.; Mishra, V. Antioxidants 2022, 11; https://doi.org/10.3390/antiox11122375
24. Hamid, A.; Haq, S.; Ur Rehman, S.; Akhter, K.; Rehman, W.; Waseem, M.; Ud Din, S.; Zain-ul-Abdin; Hafeez, M.; Khan, A.; Shah, A., Chemical Papers 2021, 75, 4189-4198; https://doi.org/10.1007/s11696-021-01650-7